Deviation Behavior Analysis and Detection Based on Flight Trajectory Data

WU Yexin, ZHAO Yifei, WANG Hongyong*

College of Air Traffic Management, Civil Aviation University of China, Tianjin 300300, P.R. China

(Received 15 May 2025; revised 20 November 2025; accepted 10 December 2025)

Abstract: Flight behavior analysis provides the fundamental basis for the future development of air traffic management (ATM). The characteristics of aircraft behavior are inherently reflected in their flight trajectories, impacting flight efficiency and safety levels. However, existing research largely addresses inefficient or abnormal trajectories from a single perspective, with an absence of a unified evaluation standard. This paper introduces a method for analyzing flight deviation behavior based on automatic dependent surveillance-broadcast (ADS-B) data, defining novel metrics of trajectory redundancy and trajectory deviation. An adaptive detection algorithm is developed to capture diverse deviation patterns. Results reveal that higher trajectory redundancy is linked to lower operational efficiency, while trajectory deviation effectively identify stepped descents, holding patterns, detours, and other behaviors. The approach offers data-driven support for anomaly detection, performance evaluation and air traffic management, with substantial significance for civil aviation applications.

Key words: deviation behavior; flight trajectory; flight safety; operational efficiency; data-driven

CLC number: V355 **Document code:** A **Article ID:** 1005-1120(2026)01-0127-18

0 Introduction

With the sustained growth of aviation traffic volume, air traffic management (ATM) have become increasing complex. There is an escalating demand for rigorous ATM performance metrics and flight operational quality assurance (FOQA). As the primary manifestation of flight behavior, the degree of trajectory compliance with standard operating procedures (SOPs) and pre-filed flight plans fundamentally dictates the safety margin of a flight. Concurrently, it also serves as a pivotal metric for quantifying airspace operational efficiency and fuel economy. Frequent practices like stepped descents and rerouting not only compromise safety levels but also delineate critical research frontiers for subsequent flight operational performance evaluations.

In accordance with general international civil aviation management procedures, a flight plan must be prepared and submitted to the ATM authority prior to departure, specifying the expected waypoints, altitudes, and estimated flight times of passage. After take-off, the actual four-dimensional (longitude, latitude, altitude and time) flight trajectory inevitably deviates from the flight plan to some extent due to pilot operations, airport approach and departure procedures, weather conditions, traffic flow, and air traffic control instructions. Guidance Material for Airplane Upset Prevention and Recovery Training (UPRT) Aid in Transport Category Airplanes issued by the Civil Aviation Administration of China (CAAC) in 2018 explicitly states that aircraft deviating from the pilot's expectation or unintentionally departing from its normal operational state can be a precursor to abnormal flight conditions[1]. Identifying such anomalies from deviations and implementing proactive safety warning is therefore of substantial practical significance and academic value.

*Corresponding author, E-mail address: yfzhao@cauc.edu.cn.

How to cite this article: WU Yexin, ZHAO Yifei, WANG Hongyong. Deviation behavior analysis and detection based on flight trajectory data[J]. Transactions of Nanjing University of Aeronautics and Astronautics, 2026,43(1):127-144.

http://dx.doi.org/10.16356/j.1005-1120.2026.01.010

On the basis of this motivation, this paper undertakes a study on flight deviation behavior. From a statistical perspective, deviation can be defined as "data that diverges from the normal data model, or fails to conform to the underlying probability distribution, or exhibits abnormal signals and magnitudes in a time series"[2]. A flight trajectory that deviates from the statistical distribution characteristics of a large set of trajectories can thus be classified as flight deviation. From an operational viewpoint, the flight plan made in advance clearly represents the pilot's expectations or normal operational states. Consequently, any divergence of the actual trajectory from the planned route can likewise be regarded as flight deviation. This paper adopts both perspectives, using either the flight plan or the historical statistical distribution of flight trajectories as the reference. To ensure evaluative equity, the reference trajectory is defined as the constrained optimal profile strictly adhering to SOPs. This definition serves to mitigate misclassification risks, preventing compliant flights from being erroneously flagged for high deviation or operational redundancy. Any flight trajectory that departs from this reference is defined as a deviation trajectory, with the deviation exceeding predetermined thresholds constituting flight deviation behavior.

Through observations of extensive historical flight trajectory data[3], it has indicated that flight deviation is characterized by frequent heading changes, resulting in denser trajectories whose overall shape becomes more complex. Compared with the typically straight and level flight paths, the trajectory with flight deviation behavior exhibits a certain degree of redundancy characteristics. In some maritime research, "redundancy" has been used to describe the density of vessel trajectories and the frequency of heading changes, with a demonstrated positive correlation between the two[4-5]. Refer to this concept, this paper introduces the metric of flight trajectory redundancy to evaluate variations of flight trajectories. When the redundancy of a target trajectory exceeds the reference trajectory redundancy by a defined threshold, the flight is considered to exhibit deviation behavior. To further quantify flight deviation magnitude, this paper firstly defines the "deviation" metric, subsequently develop an adaptive flight deviation behavior detection methodology capable of extracting behavioral differences along the entire trajectory. On this basis, a clustering algorithm is employed to determine reference trajectories, with the joint calculation of flight trajectory redundancy and deviation facilitating the identification and detection of flight deviation behaviors throughout the whole flight phase. The proposed evaluation framework of flight deviation based on flight trajectory redundancy not only advances the methodological foundations for flight behavior analysis but also provides a theoretical basis for timely anomaly detection and early warning in ATM practice.

1 Literature Review

1.1 Flight trajectory shape recognition

With the widespread deployment of automatic dependent surveillance-broadcast (ADS-B) airborne equipment and ground-based receivers[6], the acquisition of flight trajectory has become more accessible, catalyzing rapid advancement in related research. Huang et al.[7] detected aircraft loitering behavior by exploiting the continuous heading variation characteristics of trajectories, specifically identifying curved motions in the horizontal plane where cumulative heading change exceeded 360°. On this basis, Xiang et al.[8] developed an angle-symbol mapping mechanism to convert continuous heading angles into discrete directional-quadrant character sets, enabling the identification of "figure-8" loitering patterns. Based on geometric feature analysis of flight trajectories, Gingrass et al.[9] extracted key point information to determine trajectory shapes, categorizing nine standardized types, straight, detour, curved, loop, multi-loop, figure-8, out-back, switchback, sinusoidal, as well as one hybrid shape, thus achieving efficient recognition and standardized representation of multiple trajectory forms.

Shivanasab et al.[10] proposed a multi-geometric feature weighting optimization framework, illustrating that shape, orientation, and curvature constitute the primary features influencing the quality of trajectory clustering. Although these studies have primarily emphasized the extraction of flight trajectory shapes, comparatively limited attention has been given to the underlying semantic characteristics that these shapes represent.

1.2 Efficiency analysis based on flight trajectories

Flight trajectories represent the comprehensive result of a flight's operation and its interactions with external environment of multiple factors and other objects. The differences in flight distance, flight time, and even fuel consumption between two tracing points on the trajectory are unequivocal reflections of operational efficiency[11]. Guastalla[12] measured the efficiency of detour trajectories by employing the ratio of the difference between actual flight trajectories and the shortest possible trajectory to the shortest trajectory distance. Peeters et al.[13] quantified the flight efficiency of the level flight segment in the approach phase by calculating the proportion of horizontal flight distance and horizontal flight time relative to the entire descent process within the terminal area. Ma et al.[14] evaluated vertical flight efficiency during the descent process by calculating the ratio of horizontal flight distance to the total flight distance within the terminal area. Zhao et al.[15] evaluated vertical efficiency of the approach phase by utilizing vertical deviations in altitude from the optimal performance reference profile, while simultaneously quantifying horizontal efficiency through the ratio of additional approach time to unimpeded flight time. This approach successfully identified efficient continuous vertical descent behavior and inefficient step-down descent behavior. The team subsequently found the impact of detours and holding patterns on approach efficiency in the approach phase[16]. Although these studies focus on the efficiency degradation associated with step-down descents, detours, and holding patterns, they fundamentally rely on statistical methods applicable to multiple trajectories, thereby having limited applicability to analyze individual flight trajectories.

1.3 Anomaly analysis based on statistical methods

With the advancement in data-driven technologies, statistical theory-based clustering algorithms such as K-means[17] and DBSCAN[18], as well as neural network techniques like autoencoders[19-21], have been extensively applied in the anomaly analysis of flight trajectory. Das et al.[22] developed a multiple kernel based anomaly detection framework for speed anomaly detection. To address various flight conditions, Li et al.[23] proposed the ClusterAD-Flight, which employs clustering analysis to identify common patterns within datasets, where deviations from these patterns are classified as anomalies. Melnyk et al.[24] utilized clustering analysis to reveal that most abnormal flights in terminal areas involved go-around behaviors, characterized by a transition from descent to climb. Li et al.[25] introduced the concept of energy height and applied to the spectral clustering method to transform positional altitude information into energy height information, so as to quantify low-altitude anomalies of aircraft. Puranik[26] further defined energy metrics based on flight speed and altitude. Olive et al.[27] defined a bounding box encompassing trajectory sets, leveraging autoencoders for clustering and reconstruction within each box, and used reconstruction error as a criterion for flight trajectory anomaly detection. And Corrado et al.[28] integrated these indicators with operational environment and trajectory data into an autoencoder for detecting instantaneous energy anomalies in general aviation fleets. Similar to the efficiency-focused studies discussed previously, these methodologies identify speed anomalies, altitude anomalies, energy anomalies, and go-around behaviors from trajectory clusters formed by multiple flight trajectories, but are not suitable for analyzing and detecting trajectory anomalies in individual flights.

1.4 Research on pedestrian, vehicle, and vessel behaviors

In contrast to the relatively nascent field of flight behavior research, the study of behaviors related to pedestrians, vehicles, and vessels has long been an important research domain, with substantial achievements worthy for the aviation field. Regarding pedestrian behaviors, Zhu et al.[29] summarized the characteristics of pedestrian loitering behaviors in different scenarios, including single-duration dwell time, frequency of stops, and reciprocating movements within small-scale areas. Lu et al.[30] focused on metrics such as movement duration, distance-to-displacement ratio, and curvature to identify anomalous trajectories. Approaching from the scale of gait, Ding et al.[31] quantitatively analyzed stepping differences during straight-line and turning locomotion to effectively identify similar deviation behaviors. For vehicle behaviors, Sun et al.[32] detected complex loitering behaviors by calculating the cumulative rotational angles of trajectories around a centroid. Jiang et al.[33] identified hazardous vehicle behaviors such as abrupt braking and sharp turns based on trajectory motion features including direction and speed rate of change. Sun et al.[34] classified vehicle behavior as normal, leftward deviation, and rightward deviation, using lane-based reference for direction and position deviations. On this basis, He et al.[35] integrated multiple trajectory features to identify behaviors such as multiple stops and dwelling behaviors. For vessel behaviors, Zhang et al.[5] defined loitering behavior as frequent directional changes within a specific spatial range, establishing trajectory redundancy as a metric for quantifying. Li et al.[36] categorized unsafe vessel behaviors into overtaking and deviation types identifying vessel overtaking, positional deviations and speed deviations through the deviation detection model, thereby enhancing both navigational safety and efficiency. Zhou et al.[37] verified behaviors such as direct sailing, turning, and docking by using heading, turning rate, and trajectory point density. A common understanding across these studies is that metrics including trajectory redundancy, position deviation, frequent direction changes and motion index deviations reflect the behavioral characteristics of transportation objects, such as loitering, stopping, and turning behaviors. These findings provide valuable insights for advancing research on flight behavior.

Compared to research on pedestrian, vehicle, and vessel behaviors, existing studies on flight trajectories primarily rely on statistical methods for efficiency analysis and anomaly detection, with limited exploration of the specific characteristics of individual flight trajectories. Moreover, there is a lack of a unified evaluation approach. This study endeavors to analyze the spatial and motion characteristics of flight trajectories, proposing trajectory metrics capable for representing flight deviation behaviors.

2 Trajectory-Based Flight Behavior Metrics

2.1 Flight trajectory redundancy

The complete flight process from pushback at the parking stand of the departure airport to arrival at the parking stand of the destination airport can be divided into five distinct flight phases: Taxi out (from the departure stand to the takeoff runway), departure (from the takeoff runway to entering the airway), cruise (along the predetermined airway from the departure airport to the destination airport), approach (from the en-route airspace to the landing runway), and taxi in (from the landing runway to the parking stand). To minimize fuel consumption and flight time, flights are ideally conducted in straight line, level flight and continuous descent throughout each flight phase, except at designated turning waypoints. Consequently, ideal flight trajectories should comprise only of waypoint turns and straight-line flight segments. Based on this framework, this study conducted an analysis of the flight trajectories during the approach phase at Tianjin Binhai Airport, identifying two additional trajectory types beyond ideal straight-line and turning flight paths, in terms of holding patterns and step-down descents, as shown in Table 1.

Table 1 Analysis of flight operational characteristics based on trajectories

Operational characteristic	Specific indicator	Trajectory			
		Trajectory 1	Trajectory 2	Trajectory 3	Trajectory 4
Spatial distribution	Three-dimensional spatial diagram	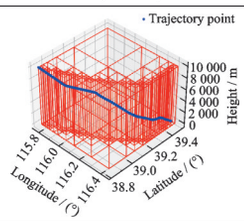	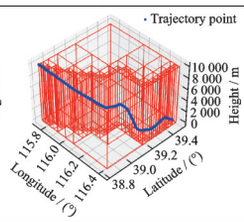	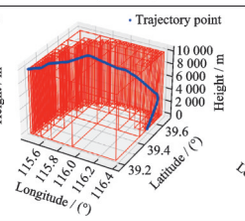	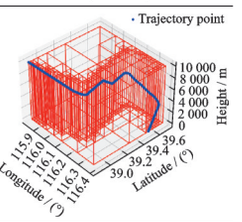
Motion patterns	Heading distribution	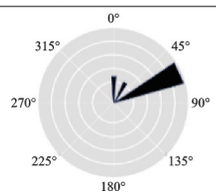	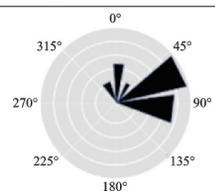	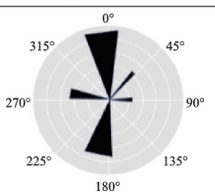	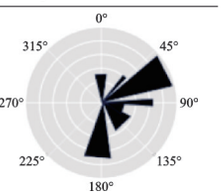
	Trajectory shapes	Straight	Sinusoidal	Switchback	Step-type vertical
Flight behaviors		Straight-line	Turning	Holding pattern	Step-down descent

As demonstrated in Table 1, a straight-line trajectory is characterized by a stable heading maintained at a fixed angle, representing a highly efficient direct-flight behavior. A sinusoidal trajectory exhibits relatively concentrated heading changes with periodic and continuous characteristics, exemplified by turning behaviors with modest angular deflections. A switchback trajectory involves frequent and substantial heading alterations, with the aircraft maneuvering within a confined airspace, such as holding patterns. A step-type vertical trajectory is primarily distinguished by segmented altitude changes, where the vertical profile displays a clear "step-like" configurations, as observed in step-down descent behaviors.

In a study on vessel behaviors, Zhang et al.[5] identified a distinctive behavior between movement and berth dwelling, specifically manifested as frequent directional changes within a confined spatial area. This behavior was defined as loitering behavior and employed "trajectory redundancy" as its quantitative characterization. This study extends this conceptual approach to the three-dimensional airspace of flight operations. As illustrated in Table 1, both the holding patterns observed in the horizontal plane and the step-down descents observed in the vertical plane can be similarly characterized through the definition of "flight trajectory redundancy".

Based on the operational characteristics of flight trajectories, this study defines a time-varying quantitative parameter $\psi(t)$, referred to as the flight trajectory redundancy. This parameter captures the dynamic changes in the spatial distribution and motion characteristics of a trajectory within time series, encompassing horizontal-plane holding patterns and vertical-plane step-down descents. Let $D_F(t)$ denote the projection length of the trajectory on plane F and $E_F(t)$ represent the perimeter of the minimum bounding rectangle of this projection (serving as a reference value for the spatial extent of flight activity). The trajectory redundancy of a flight on plane F is expressed as ψ_F, which is calculated as

$$\psi_F(t)=\frac{D_F(t)}{E_F(t)} \tag{1}$$

A flight trajectory is the temporal path of an aircraft in three-dimensional space, comprising a series of discrete trajectory points. Given a flight trajectory $S=\{P_1, P_2, \cdots, P_n\}$, each trajectory point $P_i=(x_i, y_i, z_i, t_i)$ denotes the three-dimensional spatial position of the aircraft at time t_i. Under different operational patterns, trajectories exhibiting more frequent heading variations generate correspondingly higher redundancy values. Conversely, more stable operations produce lower redundancy values, as illustrated in Fig.1. When the trajectory exhibits almost no directional change (Fig.1(a)), D becomes

significantly smaller than E, resulting in $\psi<1$. When the trajectory undergoes continuous directional variations (Fig.1(b)), D approaches E, with ψ approaches 1. When the trajectory involve persistent reciprocating directional changes within a localized spatial area (Fig.1(c)), D exceeds E, yielding $\psi>1$. Therefore, as a trajectory changing variations become more frequent, the generated trajectory length D, increases proportionally, resulting in higher trajectory redundancy ψ and corresponding greater probability of abnormal behavior occurrence.

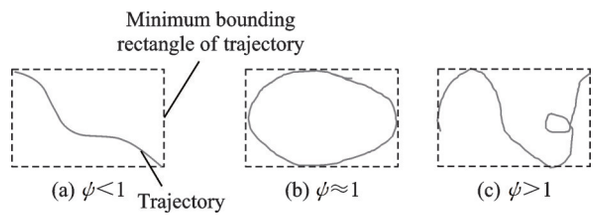

Fig.1 Comparison of redundancy for different trajectory shapes

By comparing the ratio of the projection length to its operational range in the three-dimensional space of the flight trajectory, the trajectory redundancy for each respective plane can be determined. Typical trajectory shapes on the longitude-latitude plane (F_{xy}) include straight lines, curved, loops, switchback, and sinusoidal shapes. On the longitude-altitude plane (F_{xz}) and latitude-altitude plane (F_{yz}), the primary trajectory types are straight-line and step-like configurations. Based on the specific characteristics of each flight phase, it is necessary to focus on trajectory redundancy in different planes. For instance, in the approach phase where significant altitude changes occur, the vertical profile should be the focus. During the cruise phase where altitude variations are minimal, the horizontal plane is of greater relevance.

Considering the three-dimensional attributes of flight trajectories, the flight trajectory redundancy is calculated as the weighted sum of redundancy values across the three orthogonal planes (F_{xy}, F_{xz}, F_{yz})

$$\psi(t)=\omega_1\psi_{F_{xy}}(t)+\omega_2\psi_{F_{xz}}(t)+\omega_3\psi_{F_{yz}}(t) \quad (2)$$

$$\sum_{i=1}^{3}\omega_i=1 \quad (3)$$

$$\omega_i\geqslant 0 \quad i=1,2,3 \quad (4)$$

where ω_i represents the weight for the flight trajectory redundancy index in each projection plane, and ω_1, ω_2, ω_3 correspond to the redundancy weights of planes F_{xy}, F_{xz}, F_{yz}, respectively. To ensure the interpretability and mathematical consistency of the overall redundancy metric, the weights are constrained by normalization and non-negativity conditions.

Furthermore, the weight for each plane should be adaptive rather than static, varying according to the specific objectives and contextual conditions of the evaluation. For instance, in takeoff or descent phases, redundancy in vertical trajectory profiles effectively captures flight dynamics such as altitude variation and descent gradient-parameters closely associated with fuel efficiency. Therefore, assigning higher weights to $\psi_{F_{xy}}$ and $\psi_{F_{xz}}$ facilitates more accurate evaluation of flight efficiency. Methodologically, weighting determination methods can be broadly classified into subjective and objective categories, depending on whether expert judgement or data statistics dominate the process. Compared with the former, data-driven methods offer consistency by mitigating individual biases[38]. To determine the plane-specific weights rationally, a combination weighting approach is employed with the analytic hierarchy process (AHP)[39] and the entropy wight method (EWM)[40], thereby synthesizing subjective and objective insights to obtain the combined weight for each plane. The computation is expressed as

$$\omega_i=\alpha\omega_{ci}+(1-\alpha)\omega_{ei} \quad (5)$$

where ω_{ci} and ω_{ei} denote the weights derived from AHP and EWMs, respectively; α serves as a linear weighting factor combining both to obtain the final composite weight for each plane.

(1) Weight ω_{ci} derived from AHP. The AHP is a multi-criteria decision-making (MCDM) methodology that decomposes complex problems into a goal layer, a criterion layer, and an indicator layer, assigning subjective weights based on expert knowledge and experience[39]. The main steps are as follows.

Step 1 Build the hierarchical model. Three criteria C_1, C_2, C_3 are defined to represent the tra-

jectory redundancy corresponding to the three projection planes.

Step 2 Establish the expert judgement matrix and perform pairwise comparison. Using Saaty's 1—9 scale, the relative importance of each criterion is rated to form a matrix $\boldsymbol{A}=[a_{ij}]$. The weight vector is then derived by normalizing the columns and subsequently averaging the rows.

Step 3 Check consistency verification. A consistency ratio test is applied to ensure logical coherence and acceptable consistency in expert evaluations.

(2) Weight ω_{ei} derived from EWM. EWM is an objective weighting approach where the smaller the information entropy of an indicator, the greater its influence and corresponding weight[40]. The main steps are as follows.

Step 1 Data normalization. Normalize the trajectory redundancy values of the three planes to remove dimensional inconsistencies and ensure comparability.

Step 2 Compute information entropy. Calculate the entropy values for $\psi_{F_{xy}}$, $\psi_{F_{xz}}$, $\psi_{F_{yz}}$ to quantify their informational contribution.

Step 3 Determine weights. Use the computed information entropy values to derive the redundancy weights for each trajectory plane.

2.2 Flight trajectory deviation

After establishing the redundancy metric, the aforementioned inefficient behaviors including step-down descents, holding patterns, and detours can be quantitatively represented. However, the sharp and direct descent of flight MU5375 towards the ground prior to its crash, which differed dramatically from the planned flight trajectory that maintained level flight during the en-route phase, cannot be adequately captured by this measure. To address this limitation, this study introduces the definition of flight trajectory deviation as an extension of the redundancy metric.

To quantify flight trajectory deviation, a reference trajectory is introduced. The flight trajectory deviation η is defined as the absolute value of the difference between the target trajectory redundancy ψ_{m} and the reference redundancy ψ_{c}, as expressed in Eq.(4). When this value exceeds a certain threshold, it indicates that the presence of flight deviation behavior.

$$\eta=|\psi_{\mathrm{m}}-\psi_{\mathrm{c}}| \tag{6}$$

In Eq.(6), the reference trajectory represents the ideal flight trajectory that the pilot, the airline, or the air traffic controller expects for the flight during a given phase. This trajectory is not only correlated with the flight plan, aircraft performance, airspace environment, and atmospheric conditions, but also closely associated with control procedures, airport flight procedures, traffic volume, and various other factors. Additionally, different reference trajectories can be defined for distinct flight phases. In the subsequent calculations in this paper, the trajectory that is closest to the flight plan or the shortest trajectory within the trajectory cluster serves as the reference trajectory.

When the deviation is less than or equal to the maximum acceptable deviation $\eta_{\max}$, the flight trajectory is considered as a normal trajectory

$$\eta\leqslant\eta_{\max} \tag{7}$$

where $\eta_{\max}$ represents the maximum acceptable deviation tolerated between the target flight trajectory and the reference trajectory under a specific flight phase or operational conditions. It serves as the critical threshold for distinguishing between normal and abnormal flight behavior. The selection of this value is influenced by multiple factors. In the Guidance Material for Airplane UPRT Aid in Transport Category Airplanes[1], $\eta_{\max}$ represent the parameter thresholds for deviations from normal operational states, such as airspeed, pitch angle, and roll angle. Similarly, in the flight operations quality assurance (FOQA) programs established by various airlines, alert thresholds for heading deviations, altitude deviations and other parameters also provide practical references for determining $\eta_{\max}$[41].

To comprehensively evaluate the deviation of a flight trajectory, the deviation of the entire trajectory is the maximum deviation value among all trajectory segments. By dividing the trajectory into continuous segments termly $S=\{S_1, S_2, \cdots, S_k\}$, the minimum redundancy value among the corresponding

reference trajectory segments is selected as the reference redundancy ψ_c. The deviation for each trajectory segment is then calculated, and the deviation of the entire trajectory is defined as

$$\eta_{\text{trajectory}} = \max(\eta_1, \eta_2, \cdots, \eta_k) \tag{8}$$

where $\eta_{\text{trajectory}}$ represents the deviation of the entire trajectory; and k the total number of trajectory segments. Simultaneously, the total redundancy of the entire trajectory $\psi_{\text{trajectory}}$ is defined as the sum of the redundancy values of all trajectory segments

$$\psi_{\text{trajectory}} = \psi_1 + \psi_2 + \cdots + \psi_k \tag{9}$$

The deviation metric quantifies the difference in redundancy between the actual flight trajectory and the reference trajectory, providing direct quantitative evaluation of the variance between the flight trajectory shape and the ideal operational state. Compared to existing efficiency and anomaly evaluation methods, this approach focuses on a finer granularity by analyzing the deviation of a single flight trajectory or even a specific segment of it, rather than collective multi-flight behaviors, thereby demonstrating enhanced specificity and temporal responsiveness.

3 Flight Trajectory Deviation Detection Method

As previously mentioned, a complete flight trajectory encompasses the entire process from an aircraft's pushback from the parking stand to its arrival at the destination airport's parking stand. Even for domestic regional flights, the trajectory can extend hundreds of kilometers with lasting over an hour. The crash of MU5375 was within 2 min. And earlier studies show highlights that the truly critical segments worth of attention within a trajectory are those associated with exceptional circumstances and flight phases characterized by complex flight operations, such as the approach phase. Therefore, a more practically significant deviation detection methodology involves precise segmentation of the flight trajectory to identify the trajectory segments with the most prominent deviations at an appropriate analytical scale.

An adaptive sliding time window methodology for flight deviation calculation is proposed, with the specific process outlined in Fig.2.

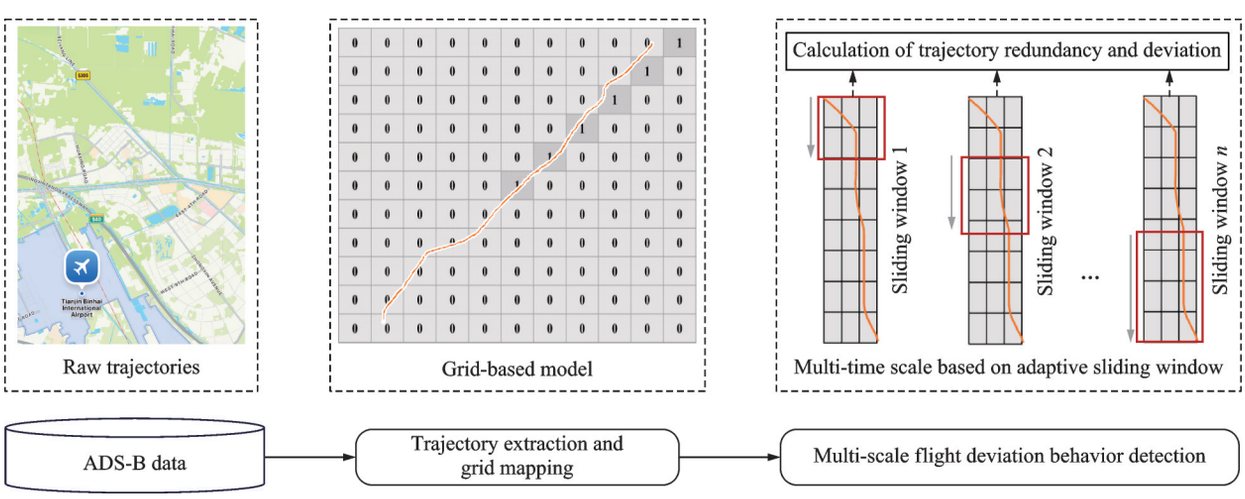

Fig.2 Flight trajectory deviation detection process

(1) ADS-B data preprocessing. The raw ADS-B data undergoes interpolation, outlier removal, and other preprocessing steps to construct a complete and continuous flight trajectory dataset.

(2) Trajectory extraction and grid mapping. Trajectory data including latitude, longitude, altitude, time, and flight number are extracted. A grid-based method is used to map the discretized flight trajectories, with grid granularity adaptively adjusted based on trajectory point density to achieve a balanced spatial distribution of data.

(3) Flight deviation behavior detection. An adaptive sliding time window is constructed, leveraging the temporal continuity characteristics of flight

trajectories to capture and detect short-time flight deviation behaviors.

3.1 Trajectory extraction and grid mapping

Considering the complexity of calculating redundancy based on the spatial characteristics of flight trajectories, this study employs a quadtree-based grid partitioning model[42], which maps the vectorized spatiotemporal coordinates of the trajectory into grid cell objects[43]. The original longitude, latitude, and altitude coordinates of the trajectory points are substituted for grid coordinates, denoted as $P(x, y, z, t) \rightarrow G(r, b, h, t)$. Each trajectory point termly p can be mapped as a grid cell object named g. Utilizing the quadtree structure, finer grid divisions are applied to areas with dense trajectory points, while coarser grid granularity is maintained in sparse regions. An independent discretization strategy is adopted to partition the vertical airspace into multiple non-overlapping altitude layers. Through combination of the horizontal grid cells with the altitude layer indices, the corresponding three-dimensional grid cell for each trajectory point is determined.

After mapping the trajectory to the grid, the redundancy detection method requires only statistical counting of grid cells traversed by the trajectory, eliminating the need to consider the exact position of the trajectory points within individual grid cells. Based on this principle, a rapid calculation method for counting grid cells traversed by trajectories is designed as

$$G_{ij} = \max(|r_i - r_j|, |b_i - b_j|) - 1 \tag{10}$$

where (r_i, b_i) represents the mapped grid position of trajectory sampling point i; (r_j, b_j) the mapped grid position of the adjacent sampling point j; and G_{ij} the minimum number of intermediate grid cells required to connect the mapped grid positions of sampling points i and j. This value can be equivalently regarded as the flight trajectory length D, which is used in the subsequent calculation of flight trajectory redundancy.

Fig.3 illustrates three typical scenarios of grid-based rapid statistics. Case 1 involves adjacent trajectory points mapped to connected grids, with the number of intermediate grids $G_{ij} = 0$. Case 2 involves adjacent trajectory points mapped to grids in the same column, with the number of intermediate grids $G_{ij} = 4$. In Case 3, the mapped grids of adjacent trajectory points are in different rows and columns, with the number of intermediate grids $G_{ij} = 3$.

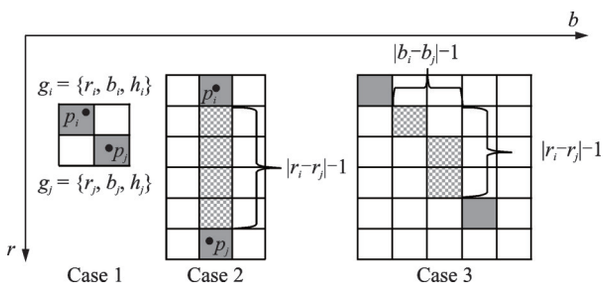

Fig.3 The least number of intermediate grids between two discrete grids (in longitude-latitude projection plane)

Therefore, a given trajectory segment S_k composed of n consecutive trajectory points is denoted as $S_k = \{p_1, p_2, \cdots, p_k\}$. Each trajectory point p_i (where $0 \leqslant i \leqslant n$) includes the flight number, the sampling time, the three-dimensional spatial coordinates (x_i, y_i, z_i) transformed into a Cartesian coordinate system, and the corresponding grid coordinates (r_i, b_i, h_i). Therefore, the trajectory point expresses as $p_i = \{\text{flight number}, t_i, x_i, y_i, z_i, r_i, b_i, h_i\}$. By sequentially calculating the intermediate grid count G_{ij} between adjacent trajectory points and accumulating these values, the number of grids traversed by the trajectory without sampling points G_w is obtained. By adding the number of grid cells that correspond to the original trajectory points G_o, the final number of grids traversed by the trajectory G_u is calculated as

$$G_w = \sum_{i=1}^{n} [\max(|r_i - r_{i+1}|, |b_i - b_{i+1}|) - 1] \tag{11}$$

$$G_u = G_o + G_w \tag{12}$$

Additionally, the number of grid cells corresponding to the bounding rectangle of trajectory segment S_k, denoted as G_v, serves as a reference for the aircraft's operational spatial range. This value is calculated as twice the sum of the number of horizontal and vertical grid cells occupied by the trajectory's bounding rectangle[4], which is equivalent to

the perimeter E of the flight trajectory's minimum bounding rectangle. Therefore, the redundancy ψ_k for this trajectory segment is the ratio of the number of grids traversed by the trajectory G_u to the number of grid cells corresponding to the minimum bounding rectangle G_v as

$$\psi_k = \frac{G_u}{G_v} \tag{13}$$

Consequently, utilizing grid count calculations for flight trajectory redundancy provides an intuitive representation of the trajectory's variation, establishing the foundation for subsequent flight behavior detection.

3.2 Flight deviation behavior detection

According to the definition of deviation, if the time scale is set too large, short-term deviations may be missed; if too small, the overall deviation may be overlooked. Therefore, an adaptive sliding time-window detection method is designed. When the trajectory redundancy exceeds the threshold or reaches the preset time limit, the trajectory is automatically segmented, enabling the comprehensive detection of flight deviation behaviors across different time scales. The adaptive principle of this method is based on a dual-trigger mechanism: When the trajectory redundancy within the sliding window exceeds the set threshold, the trajectory is immediately segmented to capture short-term deviation behaviors. If the time window reaches the preset maximum duration, the trajectory will be automatically segmented. The specific algorithm process is as follows.

Step 1 Threshold setting. The maximum time scale t_{max}, the trajectory redundancy threshold ψ_{max}, and the trajectory deviation threshold η_{max} should be specified.

Step 2 Task-create. Set the task of detecting flight deviation behaviors for trajectory S, which generates k trajectory segments. If the duration of a sliding detection window is T_k, the trajectory in this time window is $S_k = \{p_1, p_2, \cdots, p_k\}$, satisfying $t(p_k) - t(p_1) = T_k$, where the time length of the sliding window is the time difference between the first and the last trajectory points of the segment. Simultaneously, calculate the redundancy ψ_k of this trajectory segment S_k. If $\psi_k \geqslant \psi_{max}$ or $T_k \geqslant t_{max}$, the adaptive sliding time window is used for automatic trajectory segmentation.

Step 3 Reference trajectory definition. Cluster historical flight trajectory data. Within the trajectory cluster containing trajectory S, the reference trajectory is defined as the trajectory with the shortest distance to others in the cluster. The reference redundancy is the minimum redundancy of all trajectory segments in the reference trajectory.

Step 4 Trajectory segment deviation calculation. Based on the definition of flight deviation behavior, calculate the difference in redundancy between each trajectory segment of S and the reference redundancy, yielding the trajectory segment deviation η_k.

Step 5 Results merging. Generate a sequence of trajectory segments $\{S_1, S_2, \cdots, S_k\}$ with explicit time boundaries and behavior characteristics, along with their corresponding calculation results $\{\psi_1, \psi_2, \cdots, \psi_k\}$. The total redundancy of the entire trajectory is denoted as $\psi_{trajectory}$.

Step 6 Deviation behavior detection. Select the trajectory segment with the maximum deviation as the overall compliance or deviation magnitude of the entire trajectory, in terms of $\eta_{trajectory}$. If $\eta_{trajectory} > \eta_{max}$, it indicates the presence of deviation behavior in the flight.

4 Experiments and Discussion

4.1 Data processing and clustering

The ADS-B data in this study is from Tianjin Binhai International Airport (hereafter referred to as Tianjin Airport) for December 2018. The details of the ADS-B data are provided in Table 2.

According to the arrival procedures at Tianjin Airport, flights from the East China, Northwest, Southwest, and South-Central China regions approaching Tianjin Airport (TIANJIN) via VYK waypoint and flights from the Northeast and East China regions approaching via the KALBA waypoint are shown in Fig.4[44].

Table 2 Description of ADS-B data

Time	Flight number	Longitude/(°)	Latitude/(°)	Altitude/m	Head/(°)	Ground speed/knots	Vertical speed/(ft·min^{-1})
2018/12/01 12:12:00	CSC8810	117.34	39.22	2 108	178.531	147	−429

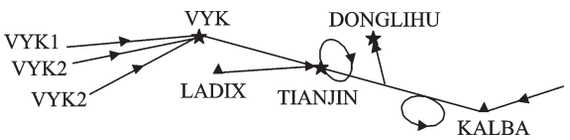

Fig.4 Arrival procedures of Tianjin Airport

The experimental area is the airspace with approximately 40 nm (74 km) radius centered on Tianjin Airport termly longitude range (116.764 1°E, 117.357 6° E) and latitude range (38.728 4° N, 39.324 1°N). A total of 120 flights landing at Tianjin Airport are collected and pre-processed, whose data size is up to about 3.38 GB.

Trajectory clustering extends standard analysis to spatio-temporal data, partitioning objectors that exhibit similar movement patterns and behaviors. Incorporating geometric similarity, this study defines a high-dimensional state space comprising five key kinematic variables: 3D position, ground speed, and heading angle. A domain-driven weighted Euclidean distance (WED) metric[45] was formulated to construct a weighted similarity model, enabling the prioritization of specific kinematic features. On this basis, considering flight consistency, a progressive density-based spatial clustering of application with noise (DBSCAN)[45] algorithm was implemented. Following fine-tuning the settings termly Eps and MinPts, the optimal configuration yielded six distinct clusters, each representing a unique flight operational pattern, as illustrated in Fig.5.

According to the arrival procedures at Tianjin Airport, the VYK1 and VYK2 arrival directions largely align with the blue cluster identified in the clustering results, whereas the VYK3 corresponds to the green cluster. The KALBA arrival direction from east to west shows four distinct trajectory clusters. Taking Cluster 1 (blue cluster) as an example, this cluster clearly contains trajectories that deviate from the standard approach path. From a vertical perspective, Fig.6(a) reveals that certain trajectories within this cluster deviate from the ideal continuous descent profile, displaying step-down descent characteristics. Such deviations are indicative of trajectory redundancy. In Fig.6(b), within the 2 000—6 000 ft (600—1 800 m) altitude block, several flights exhibit extended level or constant-

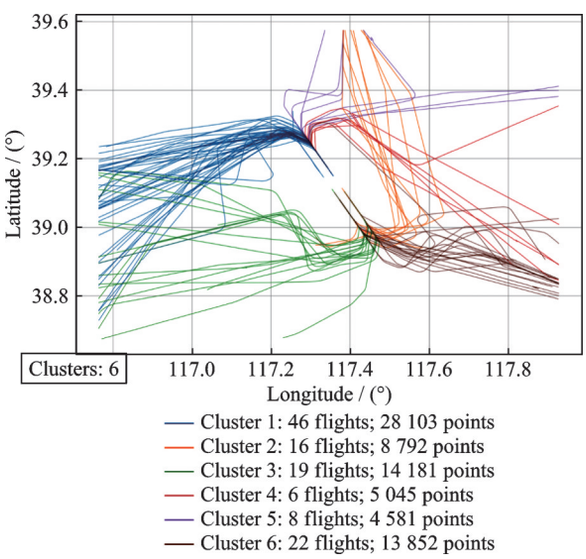

Fig.5 Clustering results of flight trajectories

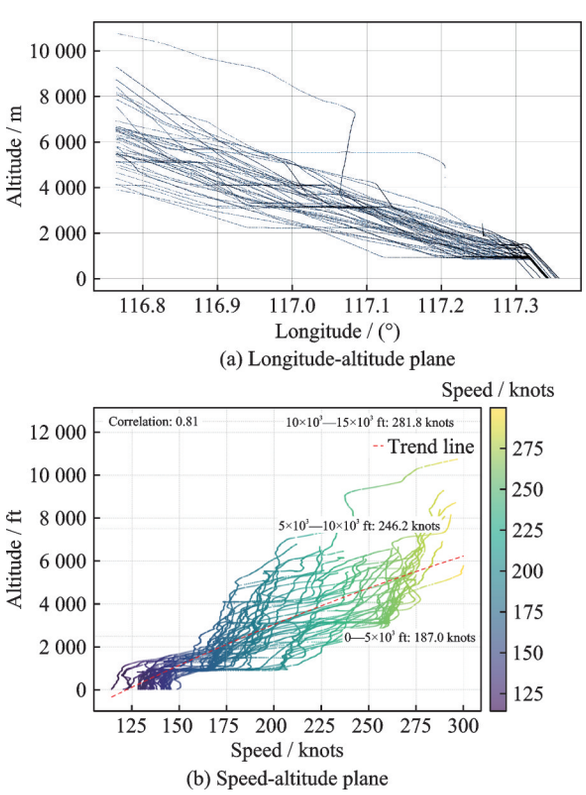

Fig.6 Vertical profile of flight trajectories in Cluster 1

rate descents. During these level flight segments, maintain airspeed required engine thrust to be greater that drag. This invariably leads to additional fuel consumption[46] and is a classic example of an inefficient flight behavior.

4.2 Calculation of flight trajectory deviation

This study selects Cluster 1 for the analysis of flight trajectory redundancy and deviation. A total of 27 820 trajectory points from 45 flights are extracted from Cluster 1. To ensure the validity of trajectory deviation analysis, the constrained optimal profile under SOPs is designated as the reference trajectory. Specific flights are identified to serve as the reference trajectories for their respective procedures. Therefore, CSC8810 and GCR7818 from VYK1 and VYK2 arrival directions are chosen. They follow all rules while completed the flight in the shortest time and distance. The trajectory redundancy threshold is set to 1, with a time threshold for the sliding window of 1 min. The combined weighting coefficient α is set to 0.5. Table 3 lists the weights of the three planes (F_{xy}, F_{xz}, F_{yz}) and the corresponding trajectory redundancy of the two reference flights.

Table 3 Weights and redundancy metrics of three planes for reference trajectories

Flight	Weight			Flight trajectory redundancy			Total
	F_{xy}	F_{xz}	F_{yz}	F_{xy}	F_{xz}	F_{yz}	
CSC8810	0.29	0.32	0.39	11.72	4.37	12.54	9.69
GCR7818				12.62	5.89	13.81	10.93

As indicated in Table 3, the combination weighting method derives weights from both expert experience and data analysis, resulting in higher weights for the two vertical planes than for the horizontal longitude-latitude plane. This finding indicates that during the approach and landing flight phase, vertical redundancy changes should be emphasized to improve the model's ability to detect and interpret flight deviations, such as step-down descent.

Table 4 presents the trajectory segments and redundancy results for the reference flight CSC 8810 in the VYK1 arrival direction.

Table 4 Redundancy analysis of flight trajectory segments for reference trajectory CSC8810

Three-dimensional trajectory redundancy analysis diagram	Segment number	Segment redundancy
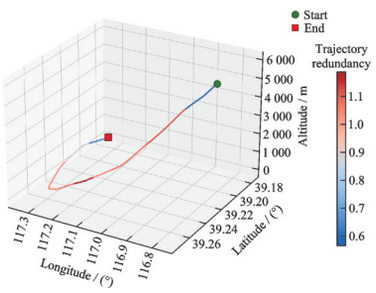	1	0.566
	2	1.124
	3	1.084
	4	1.051
	5	1.188
	6	1.081
	7	1.055
	8	1.034
	9	0.877
	10	0.629
Total trajectory redundancy		9.35

As shown in Table 4, the reference trajectory is relatively smooth, with a minimum redundancy of 0.566. This value serves as the reference redundancy to calculate the total redundancy and deviation for all flights. Table 5 summarizes the top five flights with the highest deviation. Among them, flight GCR7864 demonstrates the greatest deviation, indicating that its overall trajectory compliance is relatively poor.

Table 5 Statistical results of the top five flights with the highest deviation

Flight number	Total redundancy	Trajectory deviation
GCR7864	14.151	0.787
GCR7898	10.854	0.783
HXA2670	14.288	0.772
CQH8883	10.956	0.755
CHH7233	13.318	0.745

4.3 Results analysis

The flight trajectories of the three flights with the highest total redundancy and the three flights with the lowest total redundancy from VYK1 arrival direction in Cluster 1 are selected for comparison, as shown in Fig.7.

In Fig.7(a), the red-marked trajectory has the highest total redundancy, while the green-marked

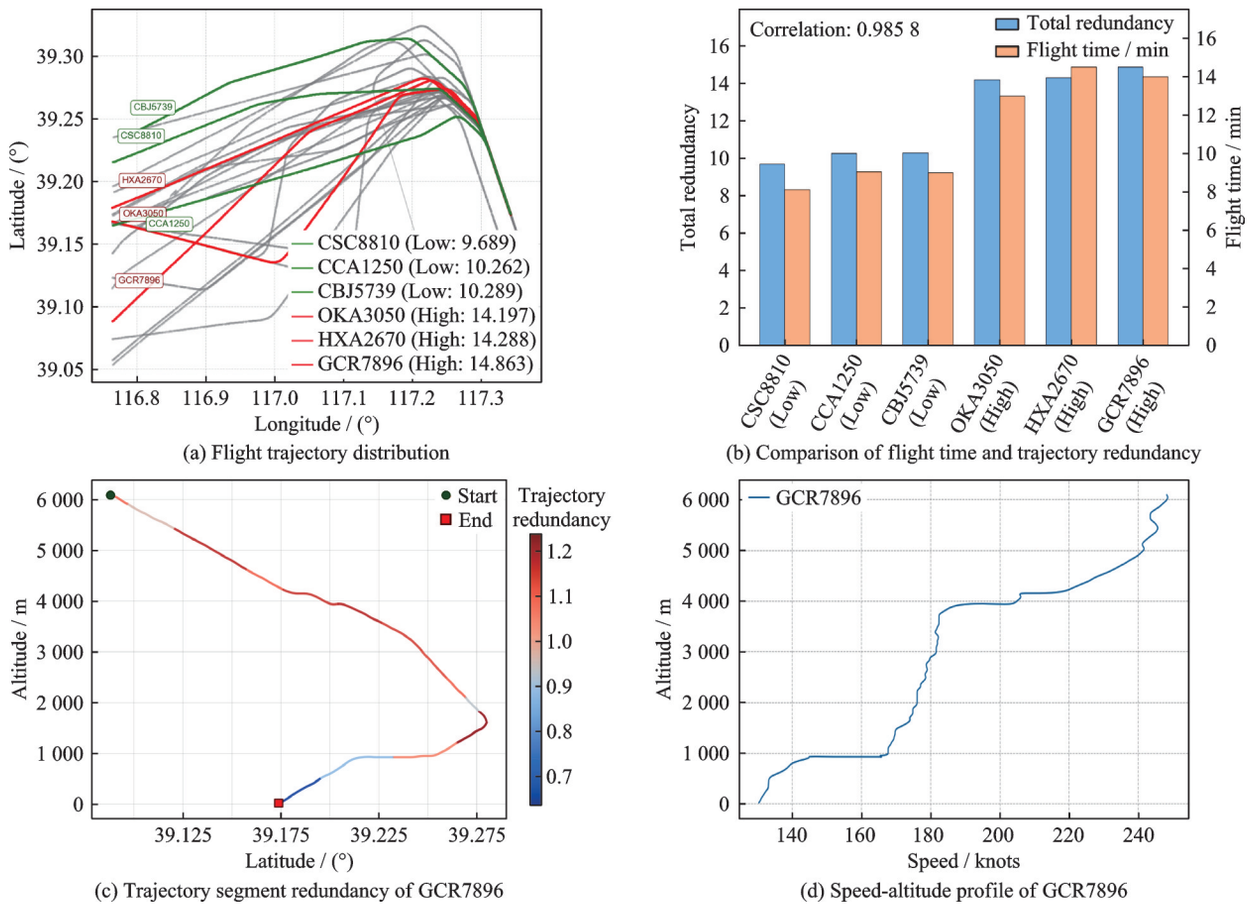

Fig.7 Flight data analysis using trajectory redundancy

trajectory has the lowest total redundancy. In Fig.7 (b), the flight time deriving from the first and last trajectory points is compared to the total trajectory redundancy, with a correlation of 0.896. It substantiates the high correlation between redundancy and flight efficiency. From the perspective of a single flight, detailed redundancy information of the trajectory is examined to gain deeper insights into trajectory inefficiencies. For the flight GCR7896 exhibiting the highest trajectory redundancy, Fig.7(c) presents its vertical projection and segmental redundancy. Fig.7(d) illustrates the speed-altitude profile, where the aircraft maintains constant speed during steep descent, leading to higher fuel consumption.

Based on the above results, it is evident that flight trajectories with higher total redundancy exhibit significant turning behaviors, longer flight times, and lower flight efficiency. This finding not only indicates that the redundancy metric designed in this study can analyze non-linear behaviors such as flight turns, but also provides a redundancy-based method for evaluating flight efficiency.

Building upon the redundancy analysis, the trajectory deviation metric enables a more precise identification of flight deviation behaviors, proving a quantitative assessment of efficiency, abnormality, and potential safety risks. As only a small subset of flights exhibits notably high deviation levels while the majority remain close to the reference trajectory, the deviation distribution within a given arrival procedure follows a non-normal pattern. Given this data distribution, the interquartile range (IQR) method[47] was employed to statistically identify deviation outliers. The 90th percentile of deviation values was set as the threshold for inefficient flights, whereas the 99th percentile was defined as the threshold for abnormal flights[46]. For the VYK1 approach, Fig.8 shows two inefficient flights (HXA2670 and GCR7898) and one abnormal flight, GCR7864, with a deviation of 0.786 847.

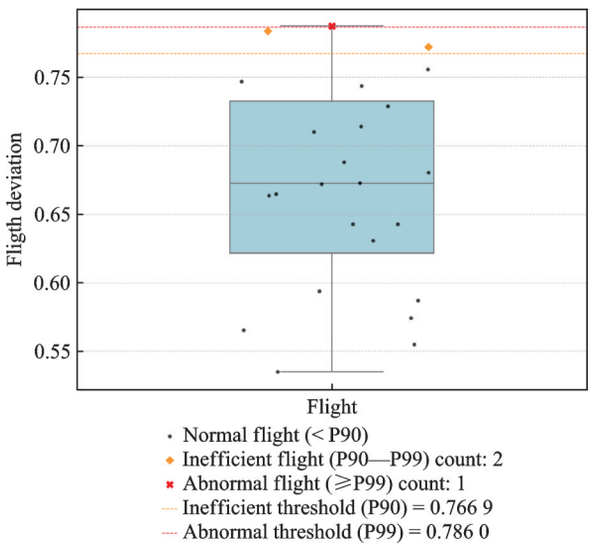

Fig.8 Flight deviation distribution in the VYK1 approach direction

Table 6 presents the deviation and redundancy analysis results for flight GCR7864, which has the highest deviation. As shown in Table 6, the trajectory segment numbered 6 exhibits significant turning behavior, with the highest deviation and relatively high redundancy.

The speed-altitude profile reveals a brief abnormal speed change near 3 000 m (segment 6 in the red-highlighted zone), possibly due to sudden weather conditions. The observed speed profile may suggest complex maneuvering. Furthermore, influenced by factors such as air traffic control (ATC) instructions, the aircraft failed to comply with the continuous descent approach (CDA) standard[48], maintaining level flight near 950 m before reducing its airspeed to approximately 140 knots (259 km/h) to initiative a stable descent. Operating under high-thrust, low-altitude, and low-speed conditions led to excessive fuel consumption and diminished safety margins. Integrating the three-plane trajectory projections reveals that the aircraft performed a step-down descent vertically and a detouring maneuver horizontally. These patterns are characteristics of inefficient and abnormal flight behaviors. Therefore, the trajectory detection method proposed in this study effectively quantifies short-term deviation behaviors, evaluates flight efficiency indicators, and identifies potential operational safety risks.

Table 6 Trajectory redundancy and deviation analysis of flight GCR7864

Three-dimensional trajectory redundancy analysis	Segment number	Segment redundancy	Segment deviation
	1	0.335	0.231
	2	1.156	0.590
	3	1.244	0.678
	4	1.064	0.498
	5	1.095	0.529
	6	1.353	0.787
	7	1.067	0.501
	8	0.992	0.426
	9	1.218	0.652
	10	1.094	0.529
	11	1.110	0.544
	12	0.849	0.283
	13	1.122	0.557
	14	0.453	0.114

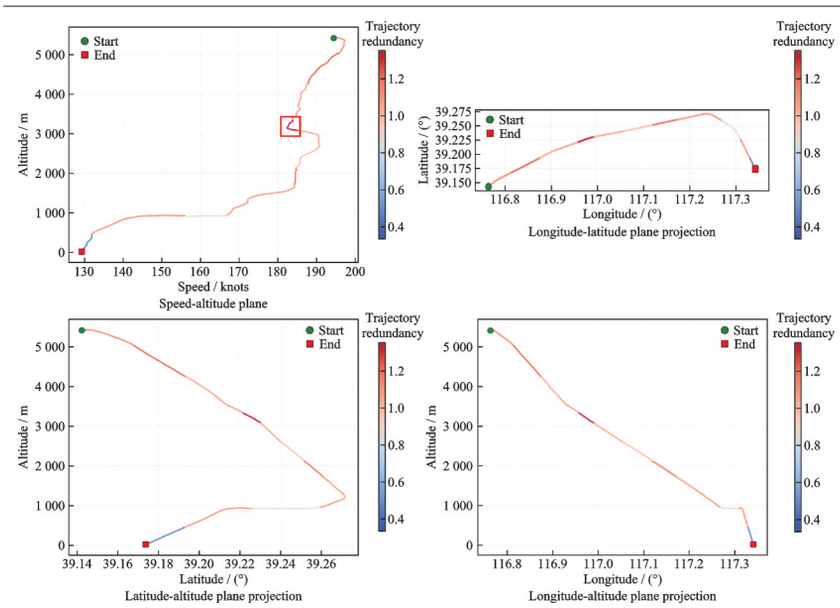

5 Conclusions

Concentrating on the limitations of existing flight behavior analysis methods in evaluating efficiency and safety, this study develops a flight deviation behavior analysis method based on ADS-B da-

ta. The main innovations are as follows.

(1) This study introduces the concepts of flight trajectory redundancy and deviation, establishing a unified framework for flight behavior evaluation. This approach overcomes the limitations of traditional methods, which typically analyzes flight efficiency or statistical anomaly detection from a single perspective.

(2) A flight behavior detection model is constructed that uses adaptive sliding time windows to automatically segment trajectories, enabling focused analysis of deviations in specific segments of the flight trajectory with enhanced specificity.

(3) A flight trajectory deviation verification methodology is deigned, capable of effectively identifying various flight deviation behaviors including step descents, detours, and holding patterns.

(4) Using actual flight data from Tianjin Airport as a case study, the positive correlation between trajectory redundancy and flight efficiency is validated, successfully identifies high-deviation flights that exhibits deviation behavior in specific trajectory segments. These findings underscore the practical application value of the method for operational efficiency and compliance with SOPs.

This paper proposes a quantitative evaluation method for flight deviation behaviors. Future research could incorporate machine learning and other advanced algorithms to improve the generalizability of this method across different airports and airspace environments, encompassing comprehensive behavioral assessment throughout all flight phases. It will contribute to the development of a more intelligent and comprehensive flight behavior evaluation system.

References

[1] Civil Aviation Administration of China. Guidance material for airplane upset prevention and recovery training aid: IB-FS—2018-013[S]. Beijing, China: Civil Aviation Administration of China, 2018. (in Chinese)

[2] BASORA L, OLIVE X, DUBOT T. Recent advances in anomaly detection methods applied to aviation[J]. Aerospace, 2019, 6(11): 6110117.

[3] Flightradar24. Live flight tracker[EB/OL]. (2025-01-30)[2025-12-08]. https://www.flightradar24.com/.

[4] HUANG Liang, WEN Yuanqiao, ZHOU Chunhui, et al. Spatiotemporal analysis methods and applications of ship trajectory big data[M]. Wuhan, China: Huazhong University of Science & Technology Press, 2024. (in Chinese)

[5] ZHANG Z H, HUANG L, PENG X, et al. Loitering behavior detection and classification of vessel movements based on trajectory shape and convolutional neural networks[J]. Ocean Engineering, 2022, 258: 111852.

[6] ZHANG Qingzhu, ZHANG Jun, LIU Wei, et al. Investigation for main problem of ADS-B implementation in ATM[J]. Measurement Control Technology and Instruments, 2007(9): 72-74.(in Chinese)

[7] HUANG Yafeng, XING Feng, ZHANG Hangfeng, et al. The research on situation assessment method based on semantic trajectories model[J]. Journal of China Academy of Electronics and Information Technology, 2019, 14(3): 243-250. (in Chinese)

[8] XIANG Longgang, GE Huiling. A direction-quadrant mapping oriented approach for trajectory moving pattern analysis[J]. Geomatics and Information Science of Wuhan University, 2020, 45(4): 495-503. (in Chinese)

[9] GINGRASS C, SINGHAM D I, ATKINSON M P. Shape analysis of flight trajectories using neural networks[J]. Journal of Aerospace Information Systems, 2021, 18(11): 762-773.

[10] SHIVANASAB P, ALI ABBASPOUR R, CHEHREGHAN A. Enhancing clustering of trajectories through optimization of geometric features[J]. Earth Science Informatics, 2025, 18(3): 275.

[11] International Civil Aviation Organization. Manual on global performance of the air navigation system: Doc 9883[S]. Montreal, Canada: International Civil Aviation Organization (ICAO), 2017.

[12] GUASTALLA G. Performance indicator-horizontal flight efficiency[R]. Brussels, Belgium: EUROCONROL Performance Review Unit, 2004.

[13] PEETERS S, GUASTALLA G. Vertical flight efficiency during climb and descent: ICNSURV—2008-8384857[R]. Brussels, Belgium: EUROCONTROL Performance Review Unit, 2016.

[14] MA Lingling, YANG Chengkai. Quantitative research on vertical flight efficiency during descent[J].

Aeronautical Computing Technique, 2018, 48(4): 41-45. (in Chinese)

[15] ZHAO Yifei, QIAO Xiaoying, QI Yancheng. The arrival efficiency of terminal area based on flight track[J]. Science Technology and Engineering, 2021, 21(13): 5575-5583. (in Chinese)

[16] ZHAO Yifei, YANG Chengkai, MA Lingling, et al. Quantization and evaluation of approach efficiency of Tianjin Binhai international airport[J]. China Sciencepaper, 2018, 13(24): 2765-2768. (in Chinese)

[17] BU Jian, ZHANG Honghai, HU Minghua, et al. Risk assessment of unmanned aerial vehicle flight based on K-means clustering algorithm[J]. Transactions of Nanjing University of Aeronautics and Astronautics, 2020, 37(2): 263-273.

[18] ZHANG W N, PAN W J, ZHU X P, et al. Identification of traffic flow spatio-temporal patterns and their associated weather factors: A case study in the terminal airspace of Hong Kong[J]. Aerospace, 2024, 11(7): 11070531.

[19] DENG Cheng, ZHANG Qiqian, ZHANG Honghai, et al. A deep learning-based approach for terminal area flight flow operational safety situation awareness[J]. Transactions of Nanjing University of Aeronautics and Astronautics, 2024, 41(6): 783-805.

[20] FAN Y Q, LIU J H, YE H, et al. TA-LSTM: A time and attribute aware LSTM for deep flight track clustering[J]. IEEE Transactions on Aerospace and Electronic Systems, 2023, 59(5): 7047-7060.

[21] LIU Y, NG K K H, CHU N N, et al. Spatiotemporal image-based flight trajectory clustering model with deep convolutional autoencoder network[J]. Journal of Aerospace Information Systems, 2023, 20(9): 575-587.

[22] DAS S, MATTHEWS B L. Multiple kernel learning for heterogeneous anomaly detection: Algorithm and aviation safety case study[C]//Proceedings of the 16th ACM SIGKDD International Conference on Knowledge Discovery and Data Mining. Washington DC, USA: ACM, 2010: 47-56.

[23] LI L S, DAS S, HANSMAN R J, et al. Analysis of flight data using clustering techniques for detecting abnormal operations[J]. Journal of Aerospace Information Systems, 2015, 12(9): 587-598.

[24] MELNYK I, BANERJEE A. A spectral algorithm for inference in hidden semi-Markov models[J]. Journal of Machine Learning Research, 2014, 18: 1-39.

[25] LI Nan, QIANG Yigeng, DENG Renbo. Research on anomaly track recognition in terminal area based on energy height[J]. Journal of Wuhan University of Technology, 2018, 40(10): 38-43. (in Chinese)

[26] PURANIK T G. A methodology for quantitative data-driven safety assessment for general aviation[D]. Atlanta, USA: Georgia Institute of Technology, 2018.

[27] OLIVE X, BASORA L. Detection and identification of significant events in historical aircraft trajectory data[J]. Transportation Research Part C: Emerging Technologies, 2020, 119: 102737.

[28] CORRADO S J, PURANIK T G, PINON-FISCHER O J, et al. Deep autoencoder for anomaly detection in terminal airspace operations[C]//Proceedings of AIAA Aviation 2021 Forum. [S.l.]: AIAA, 2021: 2405.

[29] ZHU Mengzhe, FENG Rui. Detection algorithm of pedestrian wandering based on 3D model[J]. Computer Applications and Software, 2017, 34(4): 149-156. (in Chinese)

[30] LU Jinliang, WU Guangchao, FENG Fujian, et al. Wandering recognition method based on joint trajectory features[J]. Journal of Nanjing University (Natural Science), 2021, 57(5): 724-734. (in Chinese)

[31] DING H, WANG Q, CHEN J, et al. Investigating pedestrian stepping characteristics via intrinsic trajectory[J]. Physica A: Statistical Mechanics and its Applications, 2024, 652: 130045.

[32] SUN Yuyan, SUN Limin, ZHU Hongsong, et al. Activity anomaly detection based on vehicle trajectory of automatic number plate recognition system[J]. Journal of Computer Research and Development, 2015, 52(8): 1921-1929. (in Chinese)

[33] JIANG Enyuan, WANG Xuejun. Vehicle abnormal behavior detection based on trajectory tracking[J]. Journal of Jilin University (Information Science Edition), 2016, 34(1): 98-103. (in Chinese)

[34] SUN W, ZHANG X R, ZHANG X, et al. Driving behaviour recognition based on orientation and position deviations[J]. International Journal of Sensor Networks, 2019, 30(3): 161.

[35] HE L, NIU X Z, CHEN T, et al. Spatio-temporal trajectory anomaly detection based on common sub-sequence[J]. Applied Intelligence, 2022, 52(7): 7599-7621.

[36] LI Mengxi, SHU Yaqing, ZHENG Yuanzhou, et al. Identification of unsafe behavior of ship overtaking and

deviation in bridge area[J]. Journal of Wuhan University of Technology (Transportation Science & Engineering), 2023, 47(3): 561-567. (in Chinese)

[37] ZHOU Yu, HUANG Liang, ZHOU Chunhui, et al. Classification and recognition of spatio-temporal behavior of ships based on deep learning of trajectory feature images[J]. Chine Journal of Ship Research, 2025, 20(2): 366-376.

[38] JI Zhongyuan, ZHANG Jingjing, LIU Zehao, et al. A CNN-based method for sparse SAR target classification with grad-CAM interpretation[J]. Transactions of Nanjing University of Aeronautics and Astronautics, 2025, 42(4): 525-540.

[39] WANG Lianfen, XU Shubai. An introduction to the analytic hierarchy process[M]. Beijing, China: China Renmin University Press, 1990: 2-5. (in Chinese)

[40] WANG Wenjun. Key technologies of aircraft cockpit's ergonomic design and comprehensive evaluation[D]. Xi'an, China: Northwestern Polytechnical University, 2015: 82-83. (in Chinese)

[41] ZHAO Yifei, WANG Mengqi. Important theories and critical scientific and technological questions of air traffic engineering[J]. Acta Aeronautica et Astronautica Sinica, 2022, 43(12): 26537.

[42] HUANG Liang, WEN Yuanqiao, ZHOU Chunhui, et al. Evaluation system of macroscopic marine traffic situation based on GIS and AIS[J]. Navigation of China, 2017, 40(1): 53-57. (in Chinese)

[43] ZHU Yongwen, XIE Hua, PU Fan, et al. Research of airspace gridding method and its application in air traffic management[J]. Advances in Aeronautical Science and Engineering, 2021, 12(4): 12-24. (in Chinese)

[44] Civil Aviation Administration of China. Aeronautical information publication of the People's Republic of China: MH/T 4047—2017[S]. Beijing, China: Civil Aviation Administration of China, 2017. (in Chinese)

[45] CORRADO S. A data-driven methodology to analyze air traffic management system operations within the terminal airspace[D]. Atlanta, USA: Georgia Institute of Technology, 2021.

[46] RYERSON M S, HANSEN M, BONN J. Time to burn: Flight delay, terminal efficiency, and fuel consumption in the National Airspace System[J]. Transportation Research Part A: Policy and Practice, 2014, 69: 286-298.

[47] MIYAMOTO A, LI C, VASCIK P, et al. ADS-B-based characterization of flight behaviors in terminal airspace for safety applications[C]//Proceedings of AIAA Aviation Forum and Ascend 2025. Las Vegas, USA: AIAA, 2025: 3669.

[48] International Civil Aviation Organization. Aircraft operations: Doc 8168[S]. Montreal, Canada: International Civil Aviation Organization (ICAO), 2006.

Acknowledgements This work was supported in part by the National Key Research and Development Program of China (No.2023YFB4302903), and the Fundamental Research Funds for the Central Universities (No.210525001464).

Authors

The first author Ms. **WU Yexin** received her B.S. degree in airport operation and management from Nanjing University of Aeronautics and Astronautics in 2018 and the M.S. degree in logistics and supply chain management from The University of Sydney, Sydney, Australia, in 2020. From 2022 to present, she continues pursuing the Ph.D. degree in safety science and engineering in Civil Aviation University of China, Tianjin, China. Her research is focused on flight trajectory analysis, air traffic management, and anomaly detection.

The corresponding author Prof. **ZHAO Yifei** received his B.S. degree in flight vehicle design from Northwestern Polytechnical University in 1993 and Ph.D. degree in transportation planning and management from Beihang University in 2003. He works as the dean in College of Air Traffic Management, Civil Aviation University of China in November 2019, where he is a director of the key laboratory. His research is focused on air traffic management, unmanned aircraft system traffic management, urban air mobility and relevant fields.

Author contributions Ms. **WU Yexin** designed the study, complied the models, conducted the analysis, interpreted the results, and wrote the manuscript. Prof. **ZHAO Yifei** contributed to the model component for the flight deviation detection, and supervision of the study. Prof. **WANG Hongyong** contributed to the discussion and background of the study. All authors commented on the manuscript draft and approved the submission.

Competing interests The authors declare no competing interests.

(Executive Editor: ZHANG Bei)

基于飞行轨迹数据的航班偏离行为分析与检测研究

吴烨鑫，赵嶷飞，王红勇

（中国民航大学空中交通管理学院，天津 300300，中国）

摘要：航班行为研究是未来空中交通管理的基础。航空器的行为特征直观体现在飞行轨迹上，对飞行效率和安全水平产生影响。然而，现有研究仅从单一角度对低效轨迹和异常轨迹进行分析，缺乏统一的评价标准。本文提出一种基于广播式自动相关监视（Automatic dependent surveillance-broadcast，ADS-B）数据的航班偏离行为分析方法。通过定义飞行轨迹冗余度和偏离度概念，设计开发了具有自适应性的航班行为检测方法。实验结果表明，轨迹冗余度越大，飞行效率越低。特别地，轨迹偏离度能够反映航班的阶梯下降、等待和绕飞等行为，进一步验证了方法的有效性。该研究对异常轨迹检测、飞行效率与安全评估、空中交通管理等方面提供数据支持，具有重要应用价值。

关键词：偏离行为；飞行轨迹；飞行安全；运行效率；数据驱动

研究亮点：

1. 构建了航班行为评价的统一框架。本研究创新性地引入了“飞行轨迹冗余度”与“偏离度”概念，建立了航班行为的综合评价体系。该方法有效弥补了传统研究中飞行效率分析与异常统计检测评价维度单一的局限性。

2. 实现了轨迹特征的自适应精准检测。本文研发了一种基于自适应滑动时间窗口的航班行为检测模型，实现了飞行轨迹的自动分段。该模型能够对飞行过程中的特定航段进行深度剖析，显著提升了偏离行为检测的针对性。

3. 提出了多维度的偏离行为验证方法。设计并验证了一套行之有效的飞行轨迹偏离识别方案，能够精准识别包括阶梯下降、盘旋等待在内的多种典型复杂偏离行为，为提升空管安全监视与运行效率提供了数据驱动的决策支持。